NIPPON STEEL TECHNICAL REPORT No. 94 JULY 2006

UDC 681 . 3 : 669 . 162 . 263

Development of the Visualizing Information Technique of Blast Furnace Operation

Shinroku MATSUZAKI*1 Masahiro ITO*1
Masaaki NAITO*1 Kazumoto KAKIUCHI*2
Makoto ISOBE*3 Nozomi SASAKI*4
Kenko UCHIDA*5 Harutoshi OGAI*5

Abstract

Visualization of shaft pressure variations and spatial changes caused by slipping in the blast furnace has established by turning stave temperature and shaft pressure data into images distributed in two dimensions. In addition, combining the two-dimensional distribution of secondarily processed data of changes in space and time with the progress of operation data enables early detection of shaft pressure fluctuations. It has been also found that there exists a relationship between the cohesive zone root position, assumed by the visualized two-dimensional image of the stave temperature change over time, and the origins of shaft pressure fluctuations. It is extracted quantity of characteristic namely an independ-ent ingredient from a two-dimensional image using an independent component analysis. It will be expected that spatial image and time series order become easy by watching a change of time series of independent ingredient. We have developed "Large scale database Online Modeling" as the practical method based on the Just-In-Time modeling concept on blast furnace operation, which has very complicated physical phenomena and strong non-linear specific characteristics. The validity of the developed modeling method has been confirmed by the study with blast furnace operation data, then the past similar operation data have been searched and the prospective operation data have been estimated very quickly and precisely.

1. Introduction

In operating a blast furnace, it is extremely important not only to grasp the present furnace conditions accurately but also to predict future furnace conditions as accurately as possible. As a matter of fact, in the field of iron-making, blast furnaces have been operated on a highly stable basis thanks to the operators' efforts to grasp the present furnace conditions and predict the future furnace conditions

*1 Environment and Process Technology Center
*2 Kimitsu Works
*3 Oita Works
*4 Nagoya Works
*5 Waseda University

by means of statistical analysis of actual operational data[1-4] and calculations using models[5-8] and through the application of artificial intelligence (AI)[9-14] and the application of their personal experience. However, factors that impede stable operation of blast furnaces are increasing. They include the rationalization (reduction) of manpower, the increasing use of raw materials and fuels of inferior properties, the augmentation of iron output to meet expanding demand, etc. Under these conditions, in order to secure the required productivity coefficient and decrease the consumption of reducing agents, determining various phenomena in the furnace during non-steady operation, predicting future furnace conditions and building a system for quantitatively presenting measures to take are called for more strongly than ever before.

On the other hand, recent years have seen a dramatic improvement in computer performance, diffusion of inexpensive hardware and database systems for storing large volumes of digital data, while the sophistication of digital image processing technology increases unabated. All this has made it possible to implement technologies for collecting huge volumes of blast furnace operation data in a relatively short time, storing them for prolonged periods and converting them into visual images.

In order to build a new blast furnace control system using those technologies, it is necessary to develop highly accurate continuous sensors, databases which permit storing and retrieving comprehensive blast furnace operation data, and a system which permits efficiently visualizing and analyzing the blast furnace operation data. Recently, therefore, a large-scale database was built and a technology was developed for converting blast furnace operation data into two-dimensional visual images using the database. Additionally, non-steady phenomena was analyzed in the blast furnace using the appropriate data stored in the database. This paper describes the results of those activities.

2. Database for Blast Furnace Operation Data

Nippon Steel's blast furnace database system was built in the 1980s. Since then, it had been used for some 20 years. However, since both the hardware and software of the system were obsolescent and the disk capacity was not very large, using the system to analyze non-steady blast furnace operations involved various problems. Therefore, the authors built a new database system as shown in **Fig. 1** in order to collect blast furnace operation data in as short a period as possible and analyze them on a real-time basis.

The outline of this system is as follows. Production data, blast

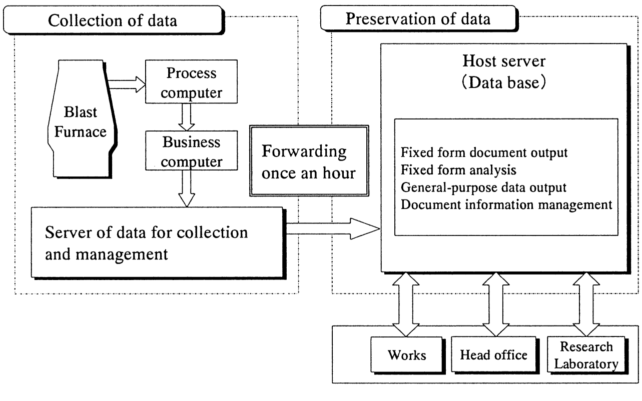

Fig. 1 Outline of data base

conditions, burden charging conditions, iron/slag tapping-related data and various types of sensor data that are collected by a process computer are compiled every minute, every hour, every day or every month according to the purpose for which they are used. Data collected from the individual blast furnaces are transmitted to a common server on an hourly basis and stored there. Basically, the authors plan to accumulate data about all of our blast furnaces for all campaigns. As a rule, the data thus accumulated can be accessed from any of the personal computers connected to the company's local area network (LAN) via the Internet.

3. System that Provides Two-Dimensional Images of Stave Temperature/Shaft Pressure Data

Despite the development of sophisticated physical models, AI and various types of probes in recent years, grasping and predicting non-steady phenomena in actual blast furnaces still depends largely on the experience and skill of the operators in the field. This is due, at least in part, to the fact that every blast furnace is provided with many different sensors. The blast furnace is a tall structure having a large inner volume. Of the many different sensors installed in the blast furnace, thermometers alone number several hundred. Organizing all the data obtained by those sensors and processing them into useful information must have required extensive experience. It is considered, therefore, that by employing a computer system to process all the sensor data, it becomes possible to utilize them more easily and more effectively. Nippon Steel has developed VENUS (Visual Evaluation and NUmerical analysis System for blast furnace operations) – a system that provides continuous, two-dimensional images of blast furnace stave temperature/shaft pressure data.

3.1 Method of two-dimensional imaging of data[15-18]

While taking the blast furnace body shape into consideration, the furnace outer profile was projected onto two-dimensional planes in vertical and horizontal directions to lay out the measured values obtained by sensors on the two-dimensional planes in such a manner that they precisely corresponded to the three-dimensional sensor installation position information to prepare equal-value, contour and vector diagrams of the measurement data. Since many of the blast furnace sensors are installed at unequal intervals, the authors developed an equal-value curve retrieval algorithm applicable to any sensor position. For any region devoid of sensors, a virtual grid appropriate to the required space resolution was set and actual measurement data obtained in its neighborhood was subjected to spatial interpolation using the actual three-dimensional Euclidean distance between the virtual grid and its nearest sensor so as to interpolate the value on the virtual grid.

1) Example of visualization of stave temperature

An example of two-dimensional visualization of stave temperature is shown in **Fig. 2**. In the figure, the horizontal axis represents the furnace azimuthal angle, the vertical axis represents the furnace height, and each asterisk (*) indicates the position of a sensor. By continuously updating the visual information, it is possible to quantify and visualize non-steady phenomena of stave temperature distribution in the furnace in an animated form.

2) Example of visualization of shaft pressure

An example of two-dimensional visualization of shaft pressure is shown in **Fig. 3**. In the figure, each arrow indicates a spatial variation vector of shaft pressure, that is, a pressure drop. It can be seen that compared with numerical data, the visual image greatly facilitates understanding of the change in shaft pressure, such as the point of occurrence of a pressure fluctuation.

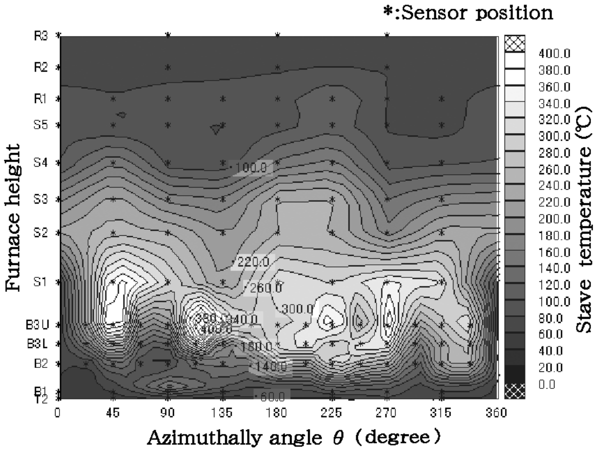

Fig. 2 Two-dimensional image of stave temperature

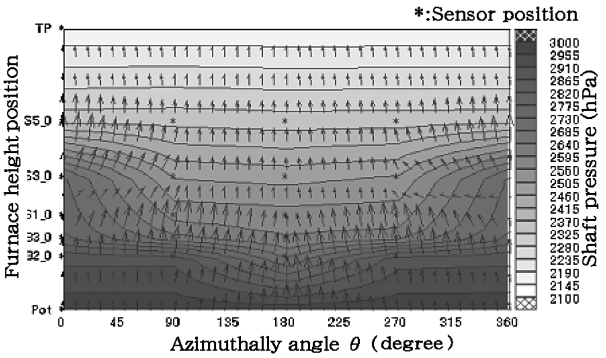

Fig. 3 Two-dimensional image of shaft pressure

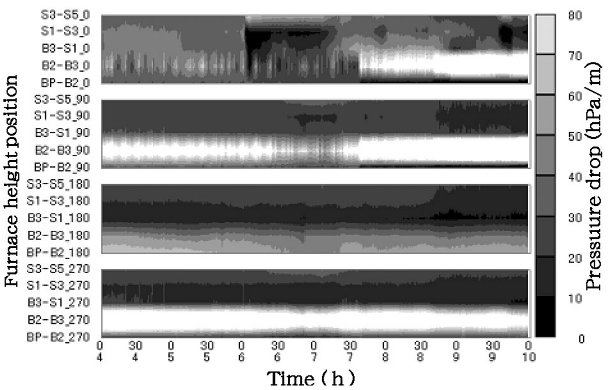

Fig. 4 Distribution of shaft pressure drop

It is considered that various phenomena that occur in the blast furnace change with the lapse of time and from space to space. Therefore, in obtaining two-dimensional images of shaft pressure, it was calculated that not only the spatial differential vector of shaft pressure but also time differential of shaft pressure taking past data into account as described in the next section.

3) Visualization of time-series changes

With two-dimensional images, like those shown in Figs. 2 and 3, it is possible to grasp the condition at a given instant but impossible to grasp the time-series change. By visualizing time-series changes in only four furnace radial directions as shown in **Fig. 4** (0, 90, 180 and 270 degrees from top down), it is possible to grasp not only the change from space to space but also the change with the lapse of time. Fig. 4 shows the time-series changes in shaft differential pressure in a vertical direction. From the figure, it can easily be seen that the shaft pressure changed at around 6:00, largely in the 0-degree direction.

By continuously visualizing (animating) data shown in Figs. 2 and 3 on the computer, it becomes possible to easily grasp the time-series changes of stave temperature and shaft pressure.

3.2 Spatial differential vector of shaft pressure

The shaft pressure sensitively reflects the changes in packing structure and gas flow in the furnace. In order to make an in-depth analysis of the pressure information, the spatial differential of shaft pressure, or the shaft pressure drop, has been monitored. The newly developed system employs a visual image of the spatial differential vector of shaft pressure, which is a generalized pressure drop, in place of the pressure drop.

As secondary processing of the visualized image of the shaft pressure, the authors defined the spatial differential vector of shaft pressure in a three-dimensional space that takes into account the bottle-shaped furnace body characteristic of the blast furnace and visualized it on two-dimensional planes projected in the vertical and horizontal directions (**Fig. 5**).

Spatial variation can be defined for stave temperature as well.

3.3 Time differential

When the gaseous or solid flows in the furnace fluctuate, the heat exchange that takes place at the furnace wall becomes markedly unstable. In addition, since the cohesive zone has poor gas permeability, when the cohesive zone changes in thickness or shape in the furnace radial direction, it is considered that the gas flow through the cohesive zone becomes uneven and the gas often tends to selectively pass through regions where the permeability resistance is smallest. In this case, it is conjectured that the transient change of the stave temperature in the region through which the gas selectively passes is greater than in other regions. Therefore, as the secondary processing of the visual image of stave temperature, the authors defined time differential and visualized it on two-dimensional planes projected in the vertical and horizontal directions. By using the time differential, it is possible to grasp the stave temperature fluctuations in the fur-

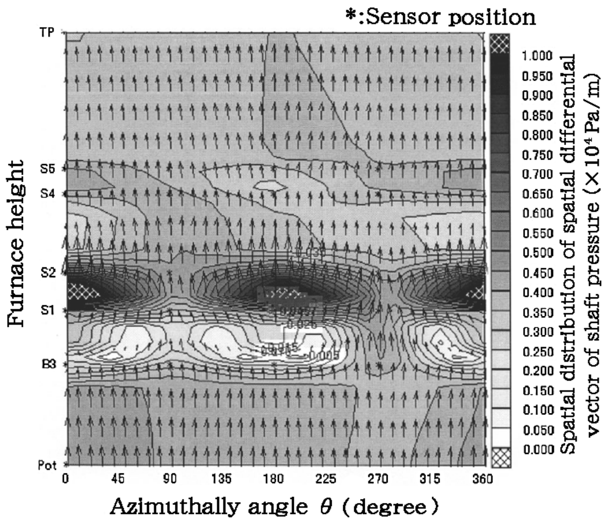

Fig. 5 Spatial distribution of spatial differential vector of shaft pressure

nace earlier and more accurately than when the measured temperatures are simply monitored. Time differential can be defined for shaft pressure as well.

As described later, it is possible to estimate the level of the cohesive zone root from the time differential of stave temperature in its visual image or from the time differential of shaft pressure, that is, the pressure drop of shaft.

Thus, by visualizing the stave temperature/shaft pressure distributions and their analytical values two-dimensionally, it becomes possible to easily grasp their spatial and transient variations in both the furnace height and furnace radial directions. In addition, it becomes possible to detect a shaft pressure fluctuation earlier and more positively than when only the probes installed at the furnace top are used.

3.4 Estimation of cohesive zone root using visual image

The authors attempted to estimate the level of the cohesive zone root using secondary-processed data in two-dimensional visual images. Various methods for estimating the cohesive zone have been reported[19-25]. They all use either the shaft pressure or the furnace body temperature. In our method of estimation using a two-dimensional visual image as well, there are two possible approaches – one using the stave temperature distribution and the other using the shaft pressure distribution.

In the method using stave temperature distribution, the cohesive zone is estimated from the time differential of stave temperature (**Fig. 6**). In the cohesive zone, the gas permeability resistance is so large that the flow of gas passing through the cohesive zone does not always become a plug flow and hence, partial out-gassing occurs frequently. As a result, at the position corresponding to the root of the cohesive zone, the stave temperature is considered to change locally. Therefore, it can be assumed that the region in which the stave temperature variation per unit time is conspicuously large is the root of the cohesive zone.

In the method using shaft pressure distribution, the cohesive zone is estimated from the spatial differential vector of the shaft pressure. Ordinarily, the pressure drop in the cohesive zone is about twice that in the shaft. In the shaft, even when the permeability decreases due to a restrained central flow, powder accumulation, etc., the gaseous flow considerably diverges and becomes uniform. In the cohesive zone root, by contrast, the gas hardly diverges laterally because of a large permeability resistance. This is considered to cause an out-gassing toward the furnace top and an abnormally large pressure drop. In other words, the pressure rise due to out-gassing plays the role of a sensor that reveals the cohesive zone. Thus, there is the possibility that the root of the cohesive zone can be determined from the position at which the pressure rises abnormally. However, since only a few shaft pressure gauges are installed in the bosh in which the cohesive zone is likely to exist because they can induce clogging, we decided to use the time differential of the stave temperature to estimate the root of the cohesive zone.

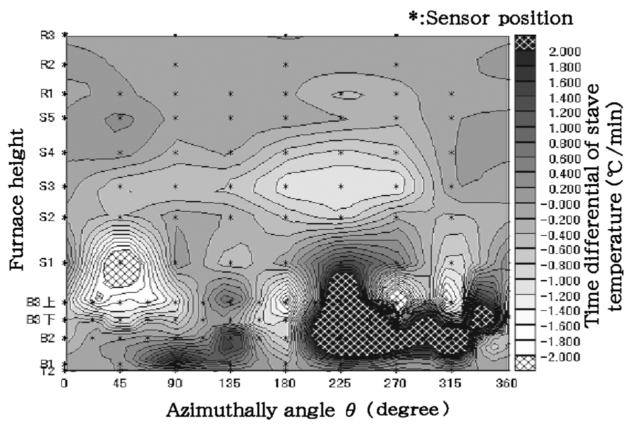

Fig. 6 Time differential of stave temperature

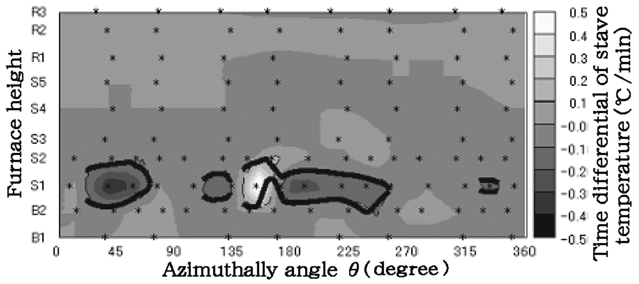

Fig. 7 Estimation result of root of cohesive zone by time differential rates of stave temperature

First, the authors prepared an equal-value diagram of time differential of stave temperatures from the stave temperature distribution. Next, a higher or lower threshold value of time differential was set and cut out patterns formed by equal-value curves of the threshold value. Then, the contours of those patterns were divided into upper and lower curves. By averaging each of the curves, the authors estimated the radial distribution of the cohesive zone root at the top and bottom, respectively[26].

It should be noted that the above method of estimation assumes that a small-scale out-gassing occurs in the neighborhood of the cohesive zone. Namely, if that phenomenon does not occur, the method is ineffective. The method cannot be applied either if a large-scale out-gassing which is not ascribable to the cohesive zone occurs since in this case, the large-scale out-gassing is detected in the first place.

An example of estimation of the root of the cohesive zone in an actual blast furnace is shown by the solid lines in **Fig. 7**. The high and low limits of time differential of stave temperatures that were used to determine the cohesive zone were ± 0.2℃/min. This criterion needs to be verified taking into consideration the actual operating condition and years of operation of the blast furnace to which the above method is applied. It can be seen from Fig. 7 that the region is assumed to be the level of the cohesive zone root can be determined, albeit partly. By tracing such a region on a time-series basis, it is possible to quantify the radial distribution of the cohesive zone root and its transient variation.

4. Pattern Analysis of Visual Images by Independent Component Analysis[27]

In order to analyze in-furnace fluctuations using visual images, it is necessary to monitor both the two-dimensional space information on the blast furnace body surface and the information on its transient change. However, it is not always easy for the operator to continually monitor them simultaneously on the CRT display of the computer system. Therefore, there was a discussion concerning extracting certain characteristic values from two-dimensional visual images, and monitor the transient changes of those characteristic values.

As the technique to extract characteristic values from visual images, independent component analysis (ICA) was adopted. In recent years, ICA is attracting attention as a method for accurately extracting the latent characteristic values in the fields of image processing and brain action signal processing. ICA consists of extracting statistically independent components from a group of multidimensional data (voice signals, visual images, etc.) and evaluating the extracted independent components, thereby quantifying the characteristics of the multidimensional data. As the ICA algorithm in the present study, we used FastICA developed by Hyvarinen et al.[28]. FastICA uses kurtosis – a forth order cumulant – to evaluate the statistical independence of each individual component.

By applying ICA to visual image $x(t)$ for a suitable period of time, it is possible to extract basic image A that represents the visual image and a dividing matrix that separates out independent component $s(t)$ that indicates how the basic images are combined to form individual images. The correlation of visual image $x(t)$, basic image A and independent component $s(t)$ can be expressed by the following equation.

$$x(t) = A\,s(t) \tag{1}$$

Basically, the number of basic images can be set arbitrarily. Assume, for example, that the number of basic images is set to five. Then, five independent components $s(t)$ are determined for the five basic images. Monitoring the changes of those independent components corresponds to monitoring animated two-dimensional images.

Fig. 8 shows five basic images, A_1-A_5 (shown at right in the figure), obtained by applying ICA (number of independent components: 5) to a group of visual images of shaft pressure in a certain blast furnace for one year, together with the transient changes of independent components, $s_1(t)$ - $s_5(t)$, for the individual basic images (the lower five rows at left in the figure) and the rates of transient variation of blast volume and shaft pressure.

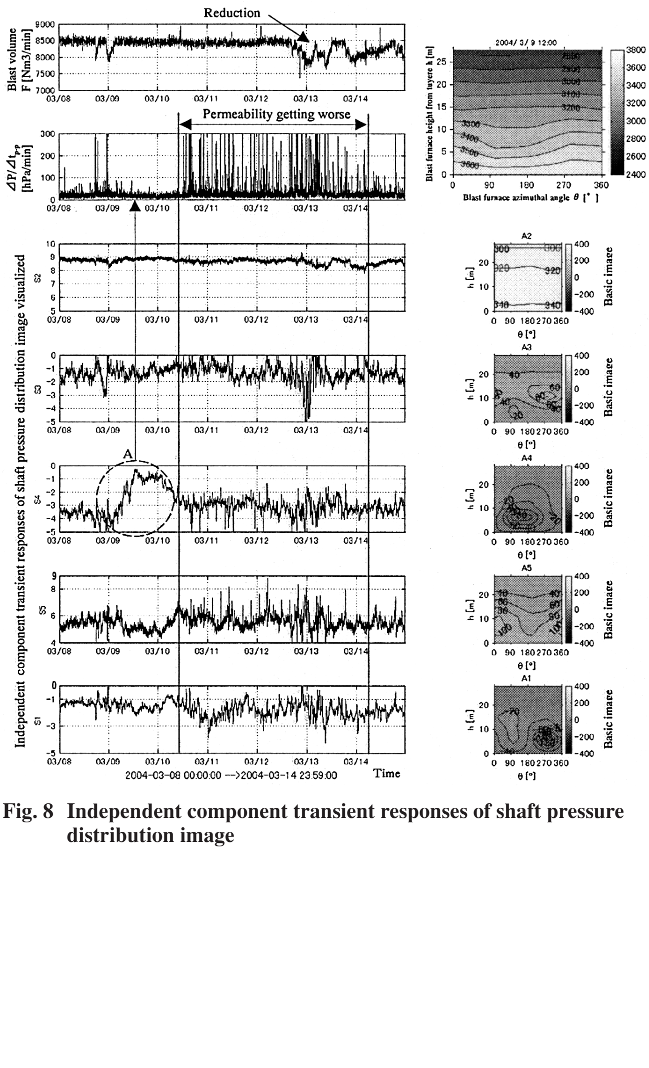

Fig. 8 Independent component transient responses of shaft pressure distribution image

Five basic images are shown here. As in the case of two-dimensional visual images of shaft pressure, the horizontal axis represents the furnace radial direction and the vertical axis represents the furnace height direction. Some of the basic images clearly show the blast furnace conditions. For example, in basic image A_2, the shaft pressure distribution in the furnace height direction is horizontal. It is considered that this image shows the basic shaft pressure distribution in a blast furnace. It is also considered that basic images A_1, A_3 and A_4 correspond to images indicating causes of pressure fluctuation, and that basic image A_5 corresponds to an image indicating the condition of pressure fluctuation. Concerning the relationship between furnace conditions and basic images, they need to be verified quantitatively in the future.

From the diagram showing the change in blast volume, it is estimated that furnace permeability began declining at around 12:00 on March 10, leading to a reduction of blast volume starting at around 18:00 on March 12. Looking at the independent components in that period, it can be seen that the independent component of basic image A_2 representing the stability of furnace operation was decreasing and that the independent components of the other basic images were fluctuating. Paying attention to independent component $S_4(t)$ that corresponds to basic image A_4, it can also be seen that it had been fluctuating markedly about a day before the furnace permeability declined (part A in Fig. 8).

As described above, by observing the transient changes of both the two-dimensional visual images and the characteristic values (independent components) extracted by independent component analysis, it should become possible to monitor the blast furnace operation both more quantitatively and more accurately.

5. Large-scale Database Online Modeling[29]

When monitoring the blast furnace operation or deciding on some action to take with the blast furnace, it is common practice to refer to relevant operational data obtained in the past or the diagram showing the change in operating condition of the furnace. Ordinarily, this retrieval of similar data obtained in the past is done based on the operator's experience and recollection. Naturally, no operator is free of human error. Therefore, in order to allow for effective utilization of relevant data obtained in the past, the authors studied the application of large-scale database online modeling technology to automate a similar data retrieval process. When this is achieved, it should become possible to predict future trends using past data.

With the progress of computer hardware and database system technology in recent years, it has become possible to accumulate huge volumes of data and retrieve necessary information from them speedily. Under that condition, local modeling techniques based on the new concept called "Just-In-Time (JIT) modeling" [30, 31] or "lazy learning" [32, 33] are attracting increasing attention. These modeling techniques work as follows. First, data obtained by observation over a wide operating range beyond the rated design points are directly stored in a database. Then, each time the need for system prediction, etc. arises, data most strongly related to the input of "query" is retrieved as "neighborhood" data from the database and a local model interpolating the output of the retrieved data is formed to obtain the output for the query.

The above new concept is characteristic in that a local model is created only when the need for system prediction, etc. arises and that after the prediction is made, the local model is discarded to allow for the accumulation of new observation data. As a rule, the choice of "neighborhood" does not depend on time, and the phase space of observation data can be expanded in order to reveal the nonlinear characteristics of the system. Case-based reasoning[34] in the field of qualitative reasoning is based on the same concept.

The problem with JIT modeling is that in order to retrieve data "neighborhood" to the "query", it is indispensable to obtain the distance between the query and each of all the observation data, and put all the data in proper order each time any system prediction, etc. is to be made. Since the blast furnace is a process (system) which is strongly characterized by complicated and nonlinear physical phenomena, a large number of observation points are set within it. Therefore, when attempting to build a large-scale database with the phase space of observation data expanded, the computation load becomes so large as to make it difficult to use the database online.

(1) Concept of retrieval of similar data obtained in the past

In the present study, therefore, a practical technique was discussed to avert the above problem in applying JIT modeling online to a large-scale database (**Fig. 9**).

This technique consists of: (1) applying a stepwise method to select only the variables that contribute to the system output from among a huge number of variables, including the phase of variables of observation data, and positively eliminate variables which can be a noise, (2) storing the observation data contained in the multidimensional phase space formed by the selected variables in a quantized database for retrieval, (3) searching the quantized database for data neighborhood to the query on a quantum-by-quantum basis to improve the efficiency of retrieval and reduce the computing load substantially, and (4) estimating the query output using a local model to interpolate the output of the retrieved similar data. This technique is the same as JIT modeling in that at the end of the estimation, the local model is discarded to allow for accumulation of new observation data so as to respond to the transient changes in the characteristics of the system to which the technique is applied.

In this paper, the above technique is termed Large scale database-based Online Modeling (LOM). An example in which LOM was applied in the operation of an actual blast furnace for its validation is shown below.

(2) Example of retrieval of similar case in the past

This is an example of retrieval of a similar case that was experienced in the past focused on the hot metal temperature. First, the data items that are considered effective for retrieval of the hot metal temperature are selected from the appropriate blast furnace operation database. Specifically, query data obtained in the past eight hours are taken out from the database, and data items that are strongly related to the hot metal temperature one hour after the query are selected from those query data using a stepwise method. Then, after all the data of the selected items are quantized and compressed, a similar case is searched for using similarity as the yardstick. As the similarity, ∞ norm was used.

$$\|X\|_\infty = \max(|X_1|, |X_2|, \cdots |X_n|) \qquad (2)$$

An example of retrieval of a similar case in the past is shown in **Fig. 10**. The figure shows the changes that were observed 48 hours before and after 0:00 that was set as the reference time for retrieval of a similar case. Namely, Fig. 10 a) shows data retrieved based on the actual hot metal temperature, and Fig. 10 b) shows the change in hot metal temperature retrieved as the similar case. It can be seen that although only eight hours of data were actually used for the retrieval, two data sets showing similar changes were retrieved in 96 hours (48 hours before and after the reference time). In Fig. 10 a), the averages of the similar data in the 48 hours after the reference time, shown in Fig. 10 b), are shown as the predicted values. It can be seen that these values also agree well with the actual values.

Concerning the actual values and one-hour predicted values, their correlation was verified using a wealth of data, including that collected in other periods. As a result, it was found that the correlation coefficient was about 0.7, indicating a relatively strong correlation (**Fig. 11**).

In order to further improve the accuracy of retrieval by our system, efforts are being made to press ahead with studies to optimize the configuration (contents and number of data items, time step, data accumulation time, etc.) of the database that is the basis for retrieval, method of selecting data from the database, number of quanta, similarity, local models, etc.

6. Conclusion

By converting stave temperature/shaft pressure data into two-dimensional visual images, it has become possible to objectively monitor the change in shaft fluctuation and spatial changes in the blast

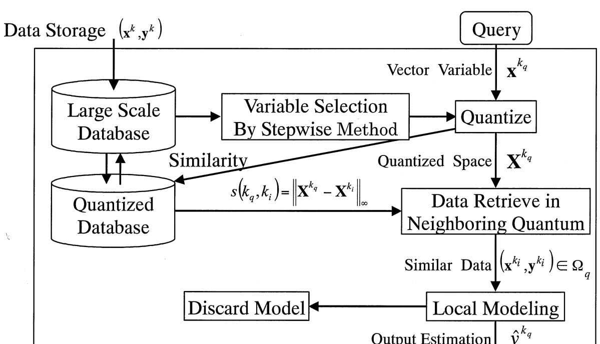

Fig. 9 Large scale database online modeling

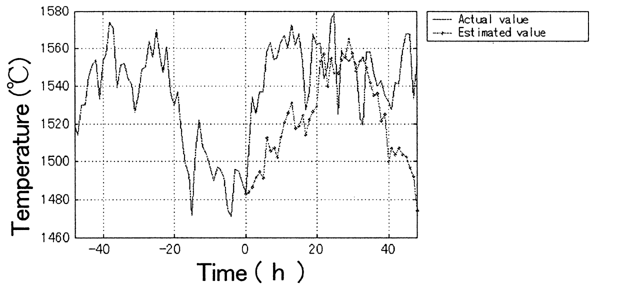

a) Actual and estimated molten iron temperature

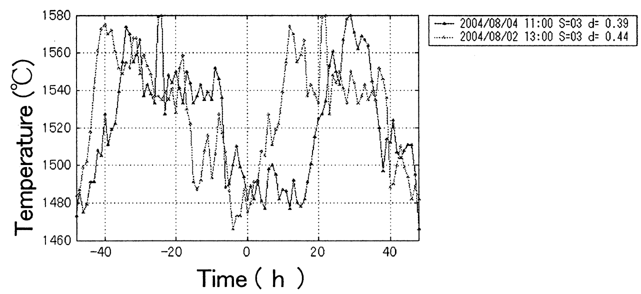

b) Actual molten iron temperature of past similar data sets

Fig.10 The past similar data sets and estimated

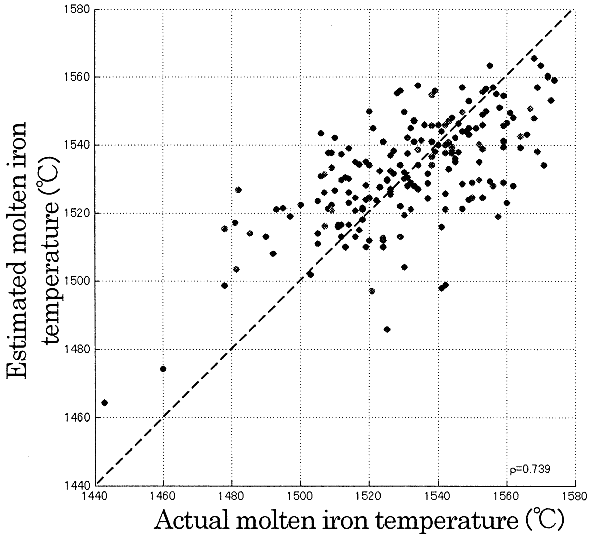

Fig.11 Correlation between after 1 hour actual molten iron temperature and estimated molten iron temperature

furnace that are caused by slipping. In addition, by observing the spatial and time differential of data and the change in blast furnace operation data at the same time, early detection of abnormal phenomena in the blast furnace is possible, such as the shaft pressure fluctuation.

Furthermore, it is expected that monitoring both the spatial and transient variations of relevant data at the same time will be facilitated by the application of independent component analysis (ICA) whereby characteristic values are extracted from visual images and their transient changes are monitored.

By using the large-scale database online modeling technique, we attempted to retrieve similar blast furnace data from data accumulated in the past. As a result, we confirmed that the technique was an effective method of data retrieval and that it would make a workable model for predicting future trends in blast furnace conditions.

References

1) Miyasaka, N., Sugata, M., Hara, Y., Kondo, S.: Tetsu-to-Hagané. 58, 18(1972)
2) Kuwano, Y., Yamamoto, S., Ohtani, K., Honda, K., Chan, T., Nakane, C.: Tetsu-to-Hagané. 58, 1203(1972)
3) Shimizu, M., Yamaguchi, A., Inaba, S., Narita, K.: Tetsu-to-Hagané. 68, 936(1982)
4) Kawata, H., Kishimoto, S., Maki, A., Saijyo, Y., Wakai, H., Yamamoto, K.: Tetsu-to-Hagané. 79, T5(1993)
5) Yagi, J.: Tetsu-to-Hagané. 69, 1242(1983)
6) Takatani, K.: Tetsu-to-Hagané. 81, 1031(1995)
7) Nogami, H.: Tetsu-to-Hagané. 89, 211(2003)
8) Sugiyama, T., Sugata, M.: Seitetsu Kenkyu. (325), 34(1987)
9) Yagi, J., Akiyama, T.: CAMP-ISIJ. 2, 2(1989)
10) Yamazaki, M., Sato, M., Kiguchi, M., Iida, O., Fukumura, S.: CAMP-ISIJ. 2, 6(1989)
11) Nagai, N., Arai, A., Matsuda, K., Kadoguchi, T., Yabata, T.: CAMP-ISIJ. 2,10(1989)
12) Otsuka, K., Matsuoka, S., Aminaga, Y., Yoshida, M., Yokoi, T., Inada, T.: CAMP-ISIJ. 2, 14(1989)
13) Takarabe, T., Nakamori, T., Oda, H., Taira, M., Watanabe, S., Seki, O.: CAMP-ISIJ. 2, 18(1989)
14) Niwa, Y., Sumikago, T., Sakurai, M., Aoki, T.: CAMP-ISIJ. 2, 22(1989)
15) Ito, M., Matsuzaki, S.: CAMP-ISIJ. 15, 927(2002)
16) Matsuzaki, S., Ito, M.: CAMP-ISIJ. 15, 928(2002)
17) Ito, M., Matsuzaki, S.: CAMP-ISIJ. 16, 300(2003)
18) Ito, M., Matsuzaki, S., Kakiuchi, K., Isobe, M.: Shinnittetsu Giho. (379), 33(2003)
19) Irita, T., Isoyama, M., Abe, T., Hasegawa, J., Okuno, Y.: Tetsu-to-Hagané. 68, S107(1982).
20) Kase, M., Sugata, M., Yamaguchi, K.: Tetsu-to-Hagané. 66, 1928(1980)
21) Ashimura, T., Morishita, N., Inoue, Y., Higuchi, M., Baba, M., Kanamori, K., Wakuri, S.: Tetsu-to-Hagané. 80, 457(1994)
22) Sasahara, S., Yamaguchi, A., Shimizu, M., Sugiyama, T., Inaba, S., Ono, R., Hachiya, S.: Tetsu-to-Hagané. 72, A5(1986)
23) Yoshida, Y., Kitayama, S., Ishiwaki, S., Nagai, N., Arai, A.: CAMP-ISIJ. 6, 49(1993)
24) Sato, T., Yamaoka, Y., Takebe, T., Kimura, R., Yamada, Y., Ohno, Y., Miyazaki, T.: Tetsu-to-Hagané. 72, A1(1986)
25) Hukushima, T., Ohno, Y., Yamada, Y., Kondo, K., Sumigame, T., Kishimoto, S.: Nippon Koukan Gihou. 99, 1(1983)
26) Ito, M., Matsuzaki, S.: CAMP-ISIJ. 16, 1109(2003)
27) Ito, M., Matsuzaki, S., Matsushita, N., Mori, J., Uchida, K., Ohgai, H.; CAMP-ISIJ. 18, 1141(2005)
28) Hyvarinen, A.: IEEE Transactions on Neural Networks. 10, 626(1999)
29) Ito, M., Matsuzaki, S., Ogai, H., Odate, N., Uchida, K., Saito, S., Sasaki, N.: Tetsu-to-Hagané. 90, 917(2004)
30) Zheng, Q., Kimura, H.: Inverse/Predictive Just in Time Controle. Private Letter. (2001)
31) Zheng, Q., Kimura, H.: Trans. Soc. Instrum. Control Eng. 37, 640(2001)
32) Atkeson, C.G., Moore, A.W., Schaal, S.: Artificial Intelligence Review. 11, 11(1997)
33) Bontempi, G., Birattari. M., Bersini, H.: Int. J. Control. 72, 643(1999)
34) Tsutsui, H., Kurosaki, A., Sato, T.: Trans. Soc. Instrum. Control Eng. 33, 947(1997)